JOURNAL OF SOLID STATE CHEMISTRY 62, 306–316 (1986)

Mechanism and Kinetics of Thermal Decompositions of Solids Governed by Phase Boundary Processes

ARMIN RELLER AND HANS-RUDOLF OSWALD

Institute for Inorganic Chemistry, University of Zürich, Winterthurerstrasse 190, 8057 Zurich, Switzerland

Received May 13, 1985; in revised form August 21, 1985

Based on structural, morphological, and thermoanalytical investigations the structural reaction mechanism including topotactic relations and the respective phase boundary process controlled macroscopic reaction mechanism of the thermal decomposition of single crystalline $Ni(SCN)_2(C_5H_5N)_2$ to $Ni(SCN)_2$ is presented. From the results obtained and from the comparison with further decomposition processes of model compounds, a general approach for the evaluation of specific kinetic parameters, in particular of direction dependent rate constants of solid state decompositions governed by phase boundary processes is derived. © 1986 Academic Press, Inc.

Introduction

The course of a thermal solid state decomposition of the type $A_{solid} \rightarrow B_{solid} + C_{gaseous}$ is characterized by compositional, structural, and morphological changes. The respective kinetic data usually are derived from the mathematical evaluation of the following equation:

$$v = d\alpha/dt = k(p, T) \cdot f(\alpha) \qquad (1)$$

where v is the reaction rate, α the fraction of decomposition ($0 \leq \alpha \leq 1$), t the reaction time, k the time- and temperature-dependent rate constant, p and T the ambient pressure and temperature, respectively, and $f(\alpha)$ an algorithm for the description of the actual macroscopic reaction mechanism (*1, 2*). The fraction of decomposition α is defined as

$$\alpha = (w_{t=0} - w_t) \cdot (w_t - w_{t=\infty})^{-1} \qquad (2)$$

where w is the sample weight at a given reaction time t.

The present contribution focusses on the experimental determination of the mechanism and the respective kinetics of the thermal decomposition of the model complex compound $Ni(SCN)_2(py)_2$ (py = C_5H_5N) to $Ni(SCN)_2$. The results obtained from structural, morphological, as well as quantitative thermoanalytical investigations yield a consistent interpretation for the mutal interdependence between microscopic and macroscopic changes occurring during the course of the decomposition. In addition, meaningful as well as reaction specific kinetic parameters are accessible.

As it will be shown, this approach leads to a general model for the mechanistic and kinetic interpretation of such complex processes.

Preparation and Thermal Behavior of Single Crystals of $Ni(SCN)_2(C_5H_5N)_2$

Stoichiometric amounts of anhydrous nickel(II) thiocyanate and pyridine were

0022-4596/86 $3.00

dissolved in a 1 : 1 : 1 mixture of methanol/ethanol/toluene. By slow evaporation of the resulting green solution at an ambient temperature of 55°C dark-green monoclinic prismatic single crystals of the solid complex were obtained. Chemical analysis of all the elements present confirmed the stoichiometric formula $Ni(SCN)_2(C_5H_5N)_2$.

The thermal behavior of $Ni(SCN)_2(py)_2$ (py $=C_5H_5N$) single crystals as well as powders were investigated on a thermomicrobalance (Perkin-Elmer TGS-2) coupled with a simultaneously working mass spectrometer (Balzers QMG 511) for the detection and identification of the gaseous products. The observed weight loss caused by the emission of molecular pyridine (Fig. 1) is in very good agreement with the theoretical values for the complete decomposition of the initial material according to the following equation:

$$Ni(SCN)_2(py)_2 \rightarrow Ni(SCN)_2 + 2(py).$$

The formation of the pure solid product $Ni(SCN)_2$ was confirmed by powder X-ray diffractometry as well as analytical determination of the elements present (*3*).

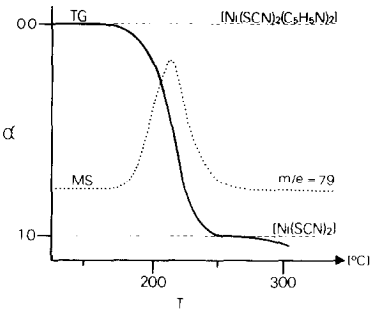

FIG. 1. Thermogravimetric and simultaneous mass spectrometric measurement of the decomposition of single crystalline $Ni(SCN)_2(py)_2$ to $Ni(SCN)_2$ under nonisothermal conditions (sample weight: 0.85 mg; heating rate: 5°/min; N_2).

The Structures of $Ni(SCN)_2(py)_2$ and $Ni(SCN)_2$

For the determination of the structural reaction mechanism as well as the characterization of elementary processes such as bond breakages and bond formations, the crystal structures of the initial material $Ni(SCN)_2(py)_2$ and the solid product $Ni(SCN)_2$ have been determined using a Picker FACS-I diffractometer with graphite monochromatized Mo$K\alpha$ radiation (λ = 0.71707 Å) (*3*, *4*).

For $Ni(SCN)_2(py)_2$ a structure made up of infinite

chains parallel to the crystallographic *c* axis of the monoclinic unit cell was found. The crystallographic data are summarized in Table I. The resulting approximately square-planar coordination of the nickel atoms by two thiocyanate sulfur atoms and two thiocyanate nitrogen atoms in trans positions is completed to a distorted octahedral coordination by two Ni–N_{py} bonds (Fig. 2). $Ni(SCN)_2(py)_2$ was found to be isostructural with $Ni(SCN)_2(NH_3)_2$ (*4*). Disorder phenomena of the arrangements of the axial pyridine ligands prevented a successful final refinement (R = 0.08). The disorder of the pyridine ligands may be ascribed to a hindered rotation around the Ni–N_{py} axis. This assumption has been reassured by the observation of superstructure reflections on Weissenberg films exposed for very long times, i.e., 24 hr and more. Due to these results the monoclinic unit cell with Z = 2 has to be transformed into a triclinic unit cell with Z = 3, within which the nickel thiocyanate chains run parallel to the space diagonal of the cell (Table I). The structural framework as such, however, remains the same. For the sake of an easier understanding of the structural changes occurring during the decomposition, the monoclinic average structure will be discussed in the following.

TABLE I

A. CRYSTALLOGRAPHIC DATA FOR THE MONOCLINIC AVERAGE-STRUCTURE AND THE TRICLINIC SUPERSTRUCTURE OF $Ni(SCN)_2(py)_2$

Crystal system	Monoclinic	Triclinic
Space group	$C2/m$	$P1$ or $P\bar{1}$
Cell dimensions	a = 9.020(5) Å	a = 8.516(2) Å
	b = 14.495(6) Å	b = 8.777(2) Å
	c = 5.573(4) Å	c = 15.365(3) Å
		α = 92.54(2)°
	β = 110.94(8)°	β = 96.57(2)°
		γ = 114.91(2)°
	V = 680.56 Å^3	V = 1029.12 Å^3
Density	ρ = 1.62 g cm^{-3} for Z = 2	ρ = 1.62 g cm^{-3} for Z = 3

B. COORDINATES OF Ni, S(SCN), C(SCN), N(SCN), AND N(py) IN THE AVERAGE STRUCTURE OF $Ni(SCN)_2(py)_2$

	Special position (space group $C2/m$)	x	y	z
Ni	2a	0	0	0
S(SCN)	4i	0.2601(1)	0	0.3496(1)
C(SCN)	4i	0.1911(3)	0	0.5929(3)
N(SCN)	4i	0.1435(3)	0	0.7644(3)
N(py)	4g	0	0.2604(3)	0

The above mentioned

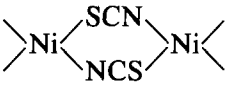

chains are characteristic features of the structural framework of $Ni(SCN)_2$ as well. In this structure, however, these chains run parallel to [110] and [1$\bar{1}$0], respectively. The Ni–N_{py} bonds are substituted by the formation of Ni–S bonds thus leading to a cross-linking of the initial parallel nickel thiocyanate chains. The resulting structure, therefore, is made up of nickel thiocyanate layers, within which the nickel atoms are mutually linked by

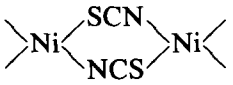

and

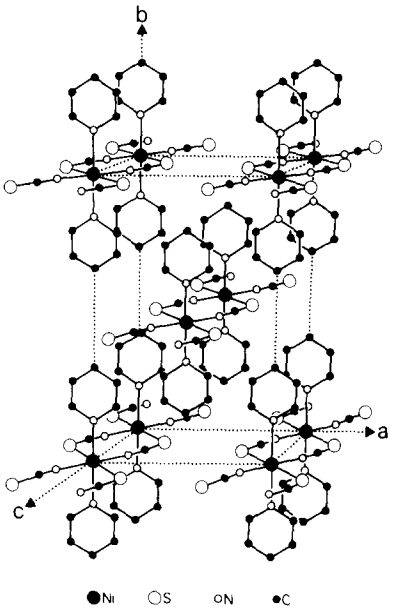

FIG. 2. Representation of the monoclinic average structure of $Ni(SCN)_2(py)_2$.

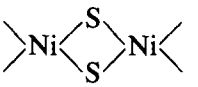

bridges (Fig. 3) (*4*).

Structural Reaction Mechanism and Topotactice Relations

X-ray diffraction patterns registered on a Weissenberg camera of fully decomposed $Ni(SCN)_2(py)_2$ single crystals, i.e., pseudo-

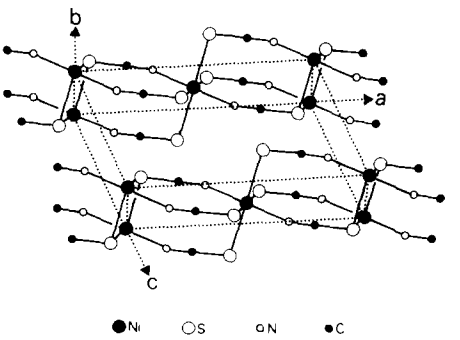

FIG. 3. Representation of the monoclinic structure of $Ni(SCN)_2$.

morphs, indicated the formation of microcrystalline but highly orientated product phase $Ni(SCN)_2$. Detailed analysis of diffraction patterns using partially decomposed $Ni(SCN)_2(py)_2$ single crystals (with $\alpha = 0.5$), which were mounted along the c axis of $Ni(SCN)_2(py)_2$ revealed, that the superimposed, parallelly arranged reflections of the product phase $Ni(SCN)_2$ correspond to the Ni–Ni distances within the thiocyanate chains again, i.e., the orientation of the thiocyanate chains [001] of the initial material is fully preserved within the product phase. Respective diffraction patterns, i.e., superimpositions of the $hk0_{Ni(SCN)_2(py)_2}$ patterns with the reflections of the product phase $Ni(SCN)_2$ gave evidence for the following crystallographic orientation relations between initial phase and decomposed phase $Ni(SCN)_2$:

$$(110)_{Ni(SCN)_2(py)_2} \parallel (001)_{Ni(SCN)_2}$$

$$(1\bar{1}0)_{Ni(SCN)_2(py)_2} \parallel (001)_{Ni(SCN)_2}$$

The formation of apparently twinned product phase pseudomorphs, which has been observed by the aforementioned X-ray diffraction experiments, can be rationalized by the transition states schematically presented in Fig. 4a and has to be explained as follows: In a first step the Ni–N_{py} bond

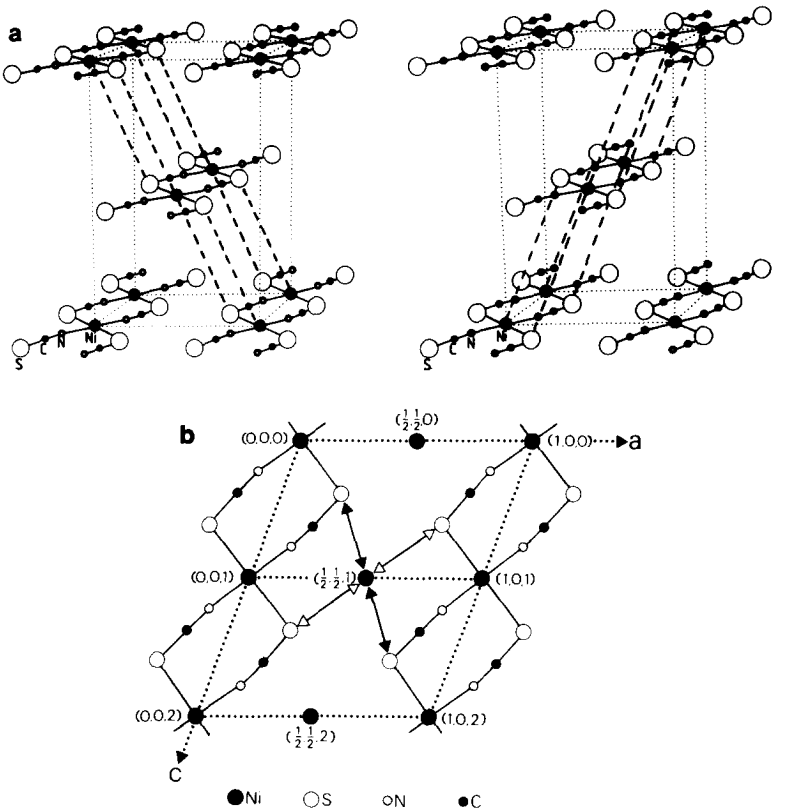

FIG. 4. (a) Hypothetical transition state in the thermal decomposition of $Ni(SCN)_2(py)_2$: Pyridine ligands are removed; the dashed lines indicate the formation of $Ni–S_{SCN}$ bonds leading to the layered structure of $Ni(SCN)_2$. (b) Schematic representation of the possible $Ni–S_{SCN}$ bond formations with respect to the structure of $Ni(SCN)_2(py)_2$ (numbers in parentheses represent the coordinates x, y, and z of the nickel atoms within $Ni(SCN)_2(py)_2$).

gets broken. In principal the free gaseous pyridine molecules could react with unoccupied metal sites again. Under the given conditions specified in the following part, however, the course of the reaction is characterized by a subsequent formation of bonds between nickel and sulfur of an adjacent thiocyanate chain. As it can be rationalized in Fig. 4b, two in terms of crystallography different closest sulfur sites exist; the respective distances between nickel and sulfur, however, are nearly equivalent in terms of metric arguments (7.98 Å respectively 8.03 Å). Due to this fact the experimental observation of the formation of twinned product phase within partially decomposed $Ni(SCN)_2(py)_2$ single crystals is reasonable and confirms the assumed structural reaction mechanism.

As a result of the loss of the pyridine ligands and the subsequent bond formations between adjacent nickel thiocyanate chains, the decomposition process is characterized by a substantial change of volume. This leads to the formation of the observed interstices (see following section) within the product phase. The relative orientation of the nickel thiocyanate chains, however, is fully preserved, as it has been confirmed by the aforementioned X-ray patterns of partially decomposed $Ni(SCN)_2(py)_2$ single crystals. In addition, the structure determinations of initial and product phase prove, that the Ni–Ni distances within the thiocyanate chains remain practically unaltered (Ni–Ni distance in $Ni(SCN)_2(py)_2$: 5.573 Å; Ni–Ni distance in $Ni(SCN)_2$: 5.543 Å).

These results are in agreement with the assumption given by the definition of a topotactic reaction mechanism (*5*): As result of a minimal number of bond breakages ($Ni–N_{py}$ bonds) and of minimal diffusion paths for the formation of new bonds ($Ni–S_{SCN}$ bonds) the main features of the initial structural framework are preserved within the structure of the product phase.

Morphological Studies

Extensive morphological studies by light and electron microscopy were carried out in order to get a consistent correlation between the microscopic structural reaction mechanism and the macroscopic morphological changes occurring during the course of the decomposition.

As hot stage light microscopy revealed the decomposition process of $Ni(SCN)_2(py)_2$ single crystals is initiated at the (001) respectively at the $(00\bar{1})$ planes of the monoclinic prisms. No product formation was observed at the other prominent crystallographic planes. The subsequent course of the reaction is characterized by the movement of the $Ni(SCN)_2(py)_2/Ni(SCN)_2$ phase boundary along [001] of the initial material, i.e., along the nickel thiocyanate chains into the bulk (Fig. 5).

To get more detailed information about the morphology of the phase boundary by means of scanning electron microscopy, $Ni(SCN)_2(py)_2$ single crystals were partially decomposed and subsequently transferred into water, where the highly soluble $Ni(SCN)_2$ product phase was washed out. The remaining insoluble $Ni(SCN)_2(py)_2$ interface was investigated and scanning elec-

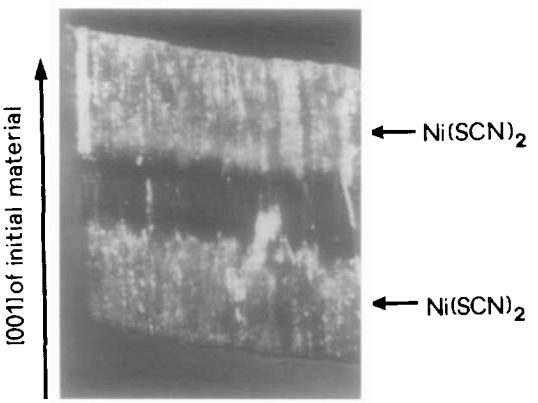

FIG. 5. Light microscopic image of a section along the direction of the nickel thiocyanate chains through a partly decomposed $Ni(SCN)_2(py)_2$ single crystal.

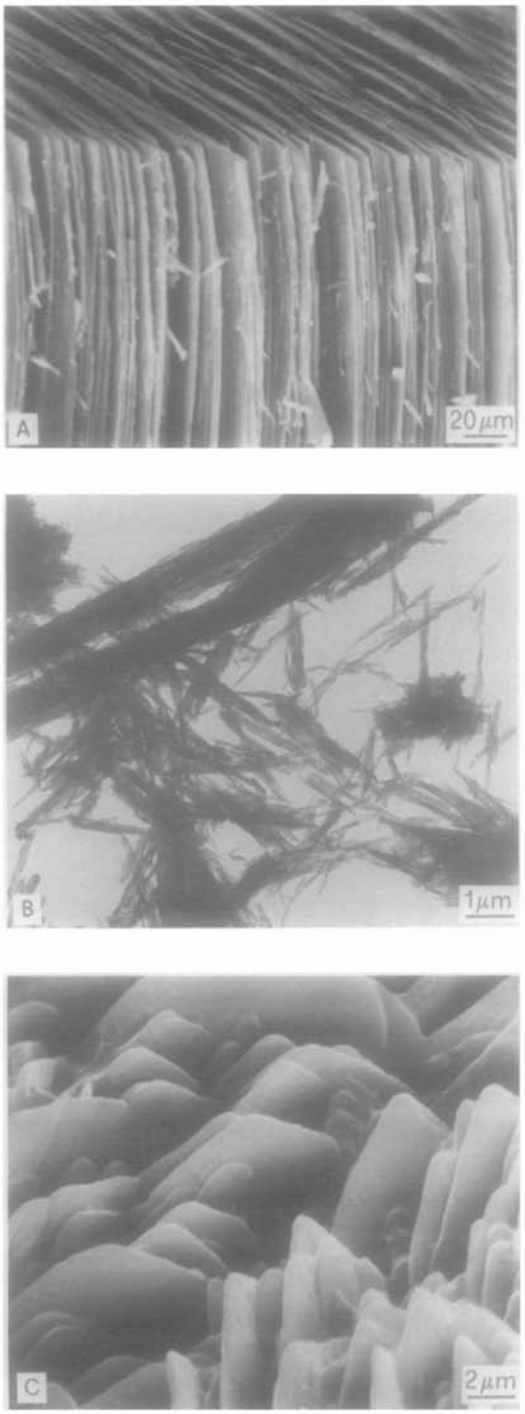

FIG. 6. (a) Scanning electron micrograph of $Ni(SCN)_2$ obtained by the decomposition of a $Ni(SCN)_2(py)_2$ single crystal. (b) Electron micrograph of dispersed $Ni(SCN)_2$ fibres obtained from the decomposition of $Ni(SCN)_2(py)_2$. (c) $Ni(SCN)_2$ crystals grown from solution (*4*).

tron micrographs showed, that the phase boundary is made up of indentations with a "bandwidth" along [001] of 2 to 3 μm within an area of about 400 μm^2 in (001) respectively $(00\bar{1})$. The "bandwidth" of the phase boundary within an isolated single crystal proved to be dependent on the actual experimental conditions such as partial pressure of pyridine, ambient pressure, and temperature distribution.

Although the parent phase boundary is not as well defined as, e.g., phase boundaries within partially reduced metal oxides (see e.g., (*6*)), its movement along $[001]_{Ni(SCN)_2(py)_2}$ could be measured with sufficient accuracy for the evaluation of respective kinetic data.

Significant reaction rates along other crystallographic directions were not observed, even if the decomposition was performed under vacuum conditions. In spite of the considerable loss of volume, fully decomposed $Ni(SCN)_2(py)_2$ single crystals were found to be well preserved pseudomorphs of the initial samples. Scanning electron microscopy gave evidence for the formation of fine $Ni(SCN)_2$ fibres (Figs. 6a,b), which are parallelly orientated. The fibre axis runs parallel to the nickel thiocyanate chains [001] of the initial $Ni(SCN)_2(py)_2$. The geometric dimensions along [001] remain nearly unaltered during the decomposition process. These facts are consistent with the conclusions derived from structural investigations. In addition, it has to be mentioned, that this fibrous habitus of the $Ni(SCN)_2$ crystallites is very unusual since this material exhibits a layered structure and, moreover, can only be synthesized from solution as single crystals with a plate-like habitus (Fig. 6c, (*4*)).

The velocity of the $Ni(SCN)_2$/

$Ni(SCN)_2(py)_2$ phase boundary movement is considerably decreased, if the (001) respectively (00$\bar{1}$) planes of the initial crystals are in direct contact with either the sample holder or with adjacent crystals, i.e., the partial pressure of pyridine represents an important parameter of the experimental set up. In Fig. 7 a model experiment is presented to give evidence for this observation: Two single crystals are set on top of each other, i.e., they are in direct contact at their (00$\bar{1}$) respectively (001) planes. The product formation is obviously hindered at the contacting planes, whereas the product formation at the "open" planes shows the normal course (see also Fig. 5). The consideration of such kind of influences are of basic importance for the evaluation of reproducible and consistent kinetic parameters (see following chapter). In addition, these observations clearly indicate that after the breakage of the $Ni–N_{py}$ bonds the volatile pyridine molecules move along the highly orientated channels of the solid product phase, i.e., along the nickel thiocyanate fibres. Subsequently, they are emitted into the ambient atmosphere at the former (001) respectively (00$\bar{1}$) planes of the initial $Ni(SCN)_2(py)_2$ single crystals.

Kinetics

For the determination of the reaction rate v and the rate constant k, respectively, quantitative time-dependent thermogravimetric measurements were carried out in flowing nitrogen (30 ml/min; 1000 mbar) and—to avoid temperature gradients and noncontrollable influences on the velocities of the phase boundary movements—under isothermal conditions in the temperature interval of 160°C + $n \cdot 5$°C (n = 0 to 8). As a consequence of the aforementioned morphological studies, all measurements were performed by using isolated (single) $Ni(SCN)_2(py)_2$ crystals with predetermined geometric dimensions between 0.175 and 0.325 mm along [001] and respective sample weights between 0.25 and 0.5 mg. To minimize the contact between sample holder

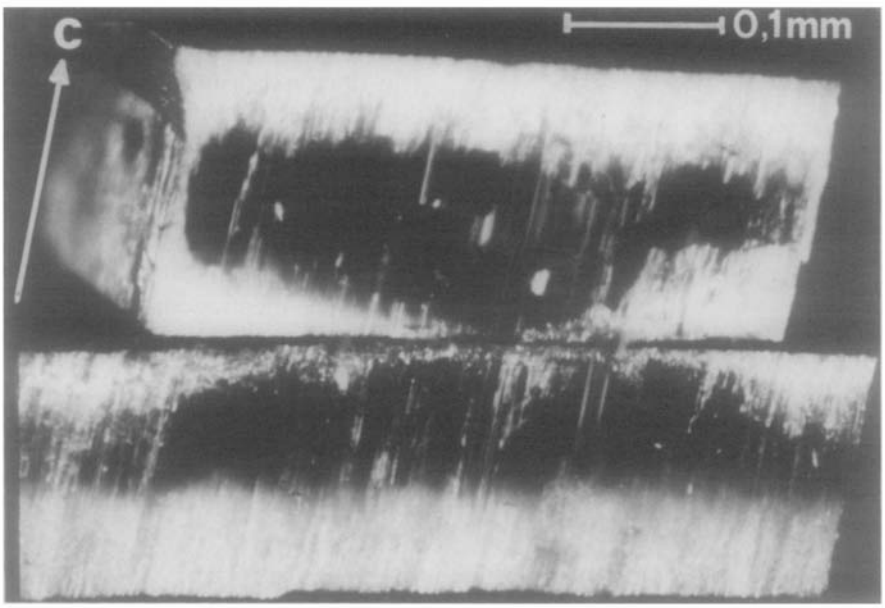

FIG. 7. Light microscopic image of a section through two partly decomposed $Ni(SCN)_2(py)_2$ single crystals, contacting each other at (001) and (00$\bar{1}$), respectively, during the course of the decomposition.

and decomposing material each crystal was mounted on a grid made up of fine platinum wires. For each temperature, at least two isolated single crystals were measured. Quantitative thermogravimetric measurements performed under the described experimental conditions gave evidence, that after a short induction period the course of the decomposition is characterized by a constant weight loss, which correlates within ±5% with the optically measured formation of the $Ni(SCN)_2$ product layers. Consequently the velocity of the $Ni(SCN)_2$/$Ni(SCN)_2(py)_2$ phase boundary movements along [001] are constant. The fact that within the temperature interval of 160 to 200°C analogous thermogravimetric and optical results (with increasing velocities) were obtained, confirmed the validity of one and the same macroscopic reaction mechanism, i.e., a one-dimensional phase boundary movement controlled mechanism. For the determination of the specific velocities along [001] summarized in Fig. 8, the thermogravimetrically measured time- and temperature-dependent reaction rates were correlated with the previously determined geometrical dimensions of the undecomposed single crystals along [001] and evaluated for the range $0.05 \leq \alpha \leq 0.85$. As an additional control, a single crystal of the initial material was covered with a thin gold film on all prominent planes except the (001) plane, i.e., the phase boundary movement only proceeded from the named plane into the crystal. Thermogravimetry revealed a constant weight loss again.

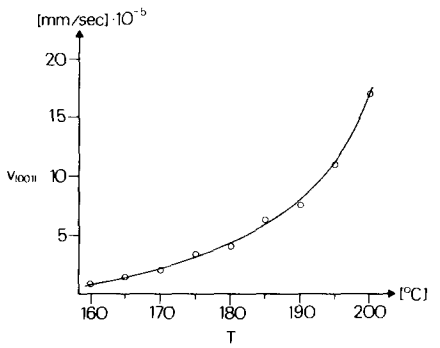

FIG. 8. Temperature versus velocity $v_{[001]}$ of the phase boundary movement for the decomposition of isolated $Ni(SCN)_2(py)_2$ single crystals.

The observation of the constant velocity $v_{[001]}$ of the advancing phase boundaries at the given temperatures and the fact, that the formation of the solid product phase, i.e., the formation of bonds between nickel and sulfur of adjacent nickel thiocyanate chains is only possible after the breakage of the $Ni–N_{py}$ bonds lead to the conclusion, that the course of the decomposition is controlled by the phase boundary process itself, i.e., by the aforementioned breakage of the $Ni–N_{py}$ bonds. If the bond formation between sulfur and nickel would be the time limiting process, one would have to expect back reactions within a relatively large area, which could not be observed experimentally. Furthermore, the formation of the product phase is favored by the minimization of the surface energy and it is reasonable to conclude, that this process is very fast.

In conclusion, a *reaction specific temperature- and direction-dependent rate constant* $k_{[001]}$ can be defined as follows:

$$k_{[001]} = v_{[001]} \cdot (c_{Ni(SCN)_2(py)_2})^{-1} \ [sec^{-1}] \quad (3)$$

where c corresponds to the crystallographic axis c of the initial material, i.e., the distance, within which $Ni–N_{py}$ bond breakages (and for that matter $Ni–S_{SCN}$ bond formations) repeatedly occur during the course of the advancing $Ni(SCN)_2/Ni(SCN)_2(py)_2$ phase boundary. In mathematical terms this specific rate constant $k_{[001]}$ represents a scalar. In Fig. 9 a $\ln k_{[001]}$ versus T^{-1} Arrhenius plot is presented. The evaluation of this plot yields an activation energy E_a of 123 ± 8 kJ/mole, which is in good agreement with the values determined by DSC measurements (*7*).

By summarizing the experimental part we conclude, that reaction specific kinetic

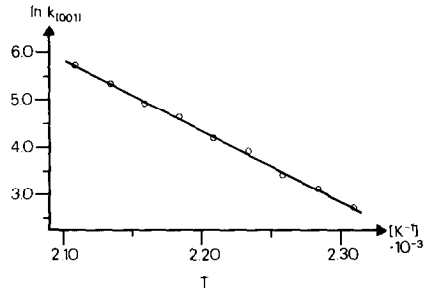

FIG. 9. $1/T$ versus $k_{\{001\}}$ Arrhenius plot for the decomposition of isolated single crystals of $Ni(SCN)_2(py)_2$ to $Ni(SCN)_2$.

data with a meaningful physico-chemical interpretation are accessible by the correlation of qualitative informations derived from compositional, structural, and morphological investigations with quantitative thermoanalytical measurements performed under well controlled conditions (see also (*8*)).

As it will be outlined in the following chapter, this kind of experimental approach to the determination of mechanism and kinetics can be generalized for solid state decompositions governed by one-, two-, or three-dimensional phase boundary movements into the initial material.

Discussion

As it has been outlined in numerous papers (see, e.g., (*2*)) kinetic investigations of decompositions of solids have been performed under isothermal or dynamic (constantly rising temperature) conditions, which yield in both cases decomposition rates of overall processes. From these quantitative measurements mostly formal kinetic parameters have been derived by mathematical algorithms, which, on their behalf, are derived from model processes governed by nucleation or diffusion. In all these procedures the fact of the governing character of the structure dependent reaction mechanism as well as morphological factors, which always are codetermining the time dependent course of a decomposition, are not taken into account. Consequently, kinetic parameters evaluated by the aforementioned procedures are not specific and reproducible quantities of a rate limiting reaction, but parameters generated by the chosen experimental setup.

The following consideration, which has been derived from the experiments presented in this paper enables the evaluation of reaction specific rate constants: The decomposition of an isolated single crystal of a compound with known composition and structure as well as with accurately predetermined structure/morphology relations leads to the formation of stable product at its surface. As it has been observed experimentally (foregoing sections, (*8*)) there exist considerable differences between the reactivities of different crystallographic planes. This fact has been observed and quantified in the field of structure and shape selectivity of solid catalysts. Moreover, different types of nucleation processes are observable as function of the actually exposed crystallographic planes.

In the case of a relatively short induction period, within which the "reacting planes" are fully covered with solid product, the subsequent course of the decomposition can be described as a specifically altered model of, e.g., B. Delmon's more general approach (*9*): From the scheme presented in Fig. 10 it follows that the fraction of decomposition

$$\alpha = \frac{V_0 - V_t}{V_0} \tag{4}$$

$$\alpha = \frac{a_0 b_0 c_0 - a_t b_t c_t}{a_0 b_0 c_0} \tag{5}$$

$$\alpha = \frac{a_0 b_0 c_0 - [(a_0 - v_a t) \cdot (b_0 - v_b t) \cdot (c_0 - v_c t)]}{a_0 b_0 c_0} \tag{6}$$

where V_0 is the volume of the initial mate-

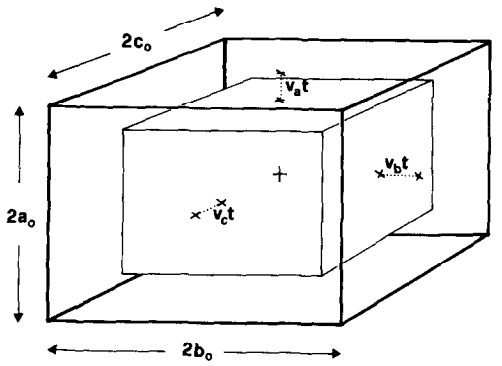

FIG. 10. Scheme representing the change of volume of the initial material as function of the velocities v_a, v_b, and v_c of the respective phase boundary movements along the coordinates a, b, and c.

rial, V_t the volume of the unreacted material at the reaction time t, $a_0/b_0/c_0$ the geometrical distances of the initial material measured from the origin of the coordinate system (in Fig. 10, +) to the respective surfaces, $a_t/b_t/c_t$ the geometrical distances of the undecomposed material at the reaction time t measured from the origin to the respective initial material/product phase boundaries, $v_a/v_b/v_c$ the velocities of the phase boundary movements along a, b, and c, respectively. The comparison of Eqs. (2) and (4) establishes the correlation between weight loss and change of volume of the reacting material. To take into account the real shape of the initial undecomposed crystal, Eq. (6) has to be multiplied with a geometry factor. Moreover, the coordinates a, b, and c have to be correlated with the actual crystallographic features.

For the evaluation of specific kinetic parameters one has to consider the fact, that the absolute values of the direction dependent velocities of the respective phase boundary movements show considerable differences, particularly in the case of highly topotactic reactions. Consequently, the relative velocities have to be known for the determination of specific rate constants even by evaluating measurements obtained from the decomposition of an isolated single crystal. Moreover, the constancy respectively nonconstancy of each phase boundary movement, i.e., of each velocity has to be checked to establish a distinctive mode between diffusion controlled and phase boundary reaction controlled decomposition. This can be effectuated by the measurement of the distances a_t, b_t, and c_t by, e.g., optical measurements using partly decomposed material at several different reaction times. Together with the knowledge of the compositional changes as well as the structural reaction mechanism, the rate-limiting step can be determined, i.e., bond breakages or diffusion of the volatile product through already formed solid product. Possible reversible reaction steps have to be taken into account. For phase boundary reaction controlled decompositions specific rate constants k finally are derived from the correlation of the velocities of phase boundary movements with the respective distances d, within which the rate limiting step of the reaction repeatedly occurs:

$$k_{(a,b,\text{ or } c)} = v_{(a,b,\text{ or } c)} \cdot d^{-1}_{(a,b,\text{ or } c)}. \qquad (7)$$

Such direction-dependent rate constants (in mathematical terms *scalars*) represent the most concise and specific kinetic parameters, which not only include the actual experimental conditions, but also the structural characteristics of the reaction.

Conclusion

Mechanism and kinetics are mutually interrelated characteristics of thermal decompositions and, more generally, of heterogeneous solid state reactions. The elucidation of the mechanistic course of such processes includes the correlation of the macroscopic morphological changes ("macroscopic reaction mechanism") with the simultaneously occurring structural rearrangements ("microscopic" or "structural

reaction mechanism"). Together with the knowledge of the concomitant compositional changes the necessary qualtitative information for the interpretation of quantitative measurements of the time, temperature, or pressure dependence of the overall process are established.

Kinetic parameters, in particular rate constants, only then represent reaction specific data, if they are interpretable in terms of the chosen experimental conditions as well as in terms of the occurring structural and compositional changes on a atomic level. Obviously and in contrast to rate constants of reactions in gases or liquids, such parameters include a defined directional component, which has to be in a relationship to the structural and/or morphological features of the reacting material. Consequently the evaluation of overall measurements, e.g., weight changes of powder-like samples or even isolated single crystals as function of time and/or temperature (*10*), cannot yield reaction specific kinetic parameters, unless the aforementioned informations derived from compositional, structural, and morphological studies are taken into account.

References

1. D. A. YOUNG, "Decomposition of Solids," Pergamon, Elmsford, N.Y., 1966.
2. W. E. BROWN, D. DOLLIMORE, AND A. K. GALWEY, "Comprehensive Chemical Kinetics" (C. H. Bamford and C. F. H. Tipper, Eds.), Vol. 22, Elsevier, Amsterdam, 1980.
3. A. RELLER, Ph.D. Thesis, University of Zürich, 1981.
4. E. DUBLER, A. RELLER, AND H. R. OSWALD, *Z. Kristallogr.* **161,** 265 (1982).
5. J. R. GÜNTER AND H. R. OSWALD, *Bull. Inst. Chem. Res. Univ. Kyoto* **42,** 505 (1970).
6. A. RELLER, J. M. THOMAS, D. A. JEFFERSON, AND M. K. UPPAL, *Proc. R. Soc. London Ser. A* **394,** 223 (1984).
7. G. B. KAUFFMANN AND G. BEECH, *Thermochim. Acta* **1,** 93 (1970).
8. H. R. OSWALD AND A. RELLER, "Materials Science Monographs" (K. Dyrek, J. Haber, and J. Nowotny, Eds.), Vol. 10(2), p. 964, Elsevier, Amsterdam, 1982.
9. B. DELMON, "Introduction à la Cinétique Hétérogène," Technip, Paris, 1969.
10. A. RELLER AND H. R. OSWALD, *J. Thermal Anal.* **29,** 1013 (1984).